*2192–2203* *Nucleic Acids Research, 2005, Vol. 33, No. 7*
*doi:10.1093/nar/gki514*

# Overexpression of Bcl-2 is associated with apoptotic resistance to the G-quadruplex ligand 12459 but is not sufficient to confer resistance to long-term senescence

**Céline Douarre[1], Dennis Gomez[1,2], Hamid Morjani[1], Jean-Marie Zahm[3], Marie-Françoise O'Donohue[4], Lahcen Eddabra[1], Patrick Mailliet[5], Jean-François Riou[1,*] and Chantal Trentesaux[1]**

[1]Laboratoire d'Onco-Pharmacologie, JE 2428, UFR de Pharmacie, Université de Reims Champagne-Ardenne, 51 rue Cognacq-Jay, 51096 Reims, France, [2]Laboratoire de Biophysique, Muséum National d'Histoire Naturelle, USM503, INSERM U565, CNRS UMR 5153, 43 rue Cuvier, 75231 Paris cedex 05, France, [3]INSERM UMR 514, CHU Maison Blanche, 45 rue Cognacq-Jay, 51092 Reims, France, [4]CNRS UMR 6142, UFR de Pharmacie, Université de Reims Champagne-Ardenne, 51 rue Cognacq-Jay, 51096, Reims, France and [5]Sanofi-Aventis SA, Département de Chimie, Centre de Recherche de Paris, 13 quai Jules Guesde, 94403 Vitry sur Seine, France

Received February 11, 2005; Revised and Accepted March 29, 2005

## ABSTRACT

**The triazine derivative 12459 is a potent G-quadruplex interacting agent that inhibits telomerase activity. This agent induces time- and dose-dependent telomere shortening, senescence-like growth arrest and apoptosis in the human A549 tumour cell line. We show here that 12459 induces a delayed apoptosis that activates the mitochondrial pathway. A549 cell lines selected for resistance to 12459 and previously characterized for an altered hTERT expression also showed Bcl-2 overexpression. Transfection of Bcl-2 into A549 cells induced a resistance to the short-term apoptotic effect triggered by 12459, suggesting that Bcl-2 is an important determinant for the activity of 12459. In sharp contrast, the Bcl-2 overexpression was not sufficient to confer resistance to the senescence-like growth arrest induced by prolonged treatment with 12459. We also show that 12459 provokes a rapid degradation of the telomeric G-overhang in conditions that paralleled the apoptosis induction. In contrast, the G-overhang degradation was not observed when apoptosis was induced by camptothecin. Bcl-2 overexpression did not modify the G-overhang degradation, suggesting that this event is an early process uncoupled from the final apoptotic pathway.**

## INTRODUCTION

Telomeres play an important role in chromosome structural integrity to cap and protect their extremities from illegitimate recombination, degradation and end-to-end fusion (1). Telomere replication is sustained in proliferative somatic cells and in most cancer cells by telomerase, a ribonucleoprotein complex that elongates the chromosome ends to compensate losses occurring at each cell division, due to the inability of polymerase to fully replicate telomeric extremities (2). In somatic cells, the absence of telomerase provokes a progressive shortening of the telomeric DNA at each round of division that ultimately leads to replicative senescence, once a critical telomere length has been reached (3). Numerous observations, notably that inhibition of telomerase activity limits tumour cell growth (4), have led to the proposition that telomere and telomerase are potential targets for cancer chemotherapy (3,5,6).

In humans, the telomere is composed of tandem repeats of the G-rich duplex sequence 5′-TTAGGG-3′, with a G-rich 3′ strand extending beyond the duplex to form a 130–210 base overhang (G-overhang) (7,8). Telomeres are believed to exist in different conformations together with several telomere-associated proteins, such as TRF1, TRF2 and Pot1 (9). The G-overhang is either accessible for telomerase extension in an open state, or inaccessible in a capped (or closed) conformation that involves the formation of a T-loop motif (9). Although the T-loop structure has not been defined in detail, it may be created by the invasion of the G-overhang into the

*To whom correspondence should be addressed. Tel: +33 3 26 91 80 13; Fax: +33 3 26 91 89 26; Email: jf.riou@univ-reims.fr

duplex part of the telomere (10). Uncapping of the telomere ends by different means leads to telomeric dysfunction characterized by end-to-end fusion, inappropriate recombination, anaphase bridges and G-overhang degradation that either lead to apoptosis or senescence (11–14).

Because of the repetition of guanines, the G-overhang is prone to form a four-stranded G-quadruplex structure that has been shown to inhibit telomerase activity *in vitro* (15,16). Small molecules that stabilize G-quadruplex are effective as telomerase inhibitors and several series of compounds have been reported to date to induce replicative senescence after long-term exposure of tumor cell cultures (17–24). Among them, the 2,4,6-triamino-1,3,5-triazine derivative 12459 (Figure 1a) is one of the most active and selective ligands that bind to the telomeric G-quadruplex. The triazine derivative 12459 was shown to induce both telomere shortening and apoptosis in the human lung adenocarcinoma A549 cell line (17). Recent results have indicated that 12459 induces short-term apoptotic effects independent of the presence of telomerase activity and that resistance to 12459 is associated with telomere capping alterations in which hTERT overexpression is essential (25). Clones selected for resistance to 12459-induced apoptosis also presented hTERT splicing alterations and/or hTERT overexpression suggesting that cellular events associated with 12459 resistance are complex (26). These resistant clones were able to maintain a high level of hTERT transcript and telomerase activity under 12459 treatment (26).

Our studies have demonstrated that another G-quadruplex ligand, telomestatin, interfered with the conformation and the length of the telomeric G-overhang, an effect that is thought to be more relevant than the double-stranded telomere erosion as a marker for telomestatin cellular activity (27). G-overhang degradation was found to be associated with the onset of senescence. Interestingly, telomestatin presented the remarkable property to remain bound to the telomere ends (27).

In an effort to better understand the mechanism(s) associated with the cellular activity of 12459, we have analyzed in this study the characteristics of the apoptosis induced by 12459 in A549 cells and the effect of this ligand on the conformation and the length of the telomeric G-overhang. Our results indicate that the apoptotic protein Bcl-2 also plays a role in the resistance to the short-term treatment of 12459. In contrast, Bcl-2 was not found to be a critical determinant of the long-term senescence induced by 12459. We also observed a rapid degradation of the telomeric G-overhang induced by short-term treatment with 12459 that paralleled the apoptotic induction, which was not observed in A549 cells undergoing apoptosis by camptothecin.

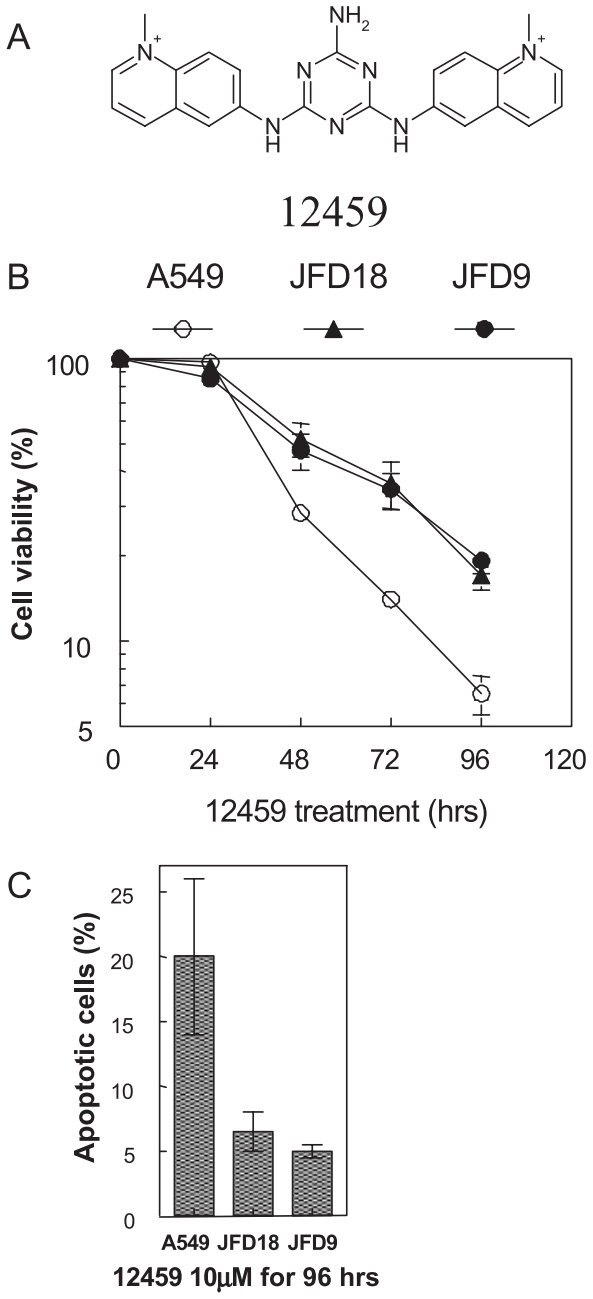


**Figure 1.** (**a**) Chemical formula of 12459. (**b**) Effect of 12459 (10 μM) on the growth of human A549 lung carcinoma parental cells, and resistant A549 cells JFD18 and JFD9 for the indicated times. Mean ± SD of triplicate independent experiments. (**c**) Apoptosis induction by 12459 (10 μM) in A549, JFD18 and JFD9 cells after 96 h of treatment. Cells were fixed and stained with Hoechst 33342, and the percentage of cells exhibiting apoptotic nuclei was calculated relative to untreated cells.

## MATERIALS AND METHODS

### Cell culture and drug treatments

Human A549 lung carcinoma cell line was obtained from the American Type Culture Collection (Rockville, MD) and 12459 resistant A549 clones, JFD18 and JFD9 were obtained as described previously (25). Cells were cultured in DMEM with Glutamax (Invitrogen) and supplemented with 10% fetal calf serum and antibiotics. A549::Bcl-2 cell line was obtained by transfection of parental A549 cells by pcDNA3Bcl-2 vector (a gift from L. Debussche, Sanofi-Aventis, Vitry sur Seine, France) with Lipofectamine$^{TM}$ 2000 kit and further selection with geneticin was done for 3 weeks.

For drug treatment, the triazine derivative 12459 (synthesized according to patent WO-0140218) was prepared in dimethyl sulfoxide (DMSO) at 10 mM. This stock solution was kept at −20°C in aliquots. Further dilutions were performed in water to be added at the appropriate concentration to cell cultures in the exponential phase of growth.

Due to an interference of 12459 with the coloration induced by MTT, the survival assay for this compound was performed in 12-well plates, each point in triplicate. The number of viable cells was counted for trypan blue dye exclusion in a hematocytometer.

Camptothecin was commercially available (Sigma) and was dissolved in DMSO at 1 mM. Further dilutions were made in water.

### Detection of apoptotic cells

Cells were grown in 12-well plates and were treated with appropriate concentrations for 1–4 days. During apoptosis, some adherent A549 cells rounded and detached themselves from the layer. Thus apoptosis was monitored on both attached and floating cells. Cells were washed with phosphate-buffered saline (PBS) and stained with Hoechst 33342 at 1 μg/ml. Cells with apoptotic morphology (cell shrinkage, nuclear chromatin condensation or apoptotic bodies) were counted in different parts of the slide by fluorescence microscopy. For camptothecin, in parallel to single-strand overhang experiments, A549 cells were grown for apoptotic evaluation. After 48 h, control cells or cells treated with 5 μM camptothecin were fixed with 5% paraformaldehyde in PBS, and then dyed with DAPI. After mounting in Citifluor (Sigma), cells were observed with an Axiovert 200M inverted microscope (Zeiss) equipped with an LD achroplan 40× objective. Images were collected with a CCD cooled camera (Coolsnap HQ, Ropper Scientific).

### Long-term culture

For long-term cell growth studies, cells were seeded at $15 \times 10^3$ cells/ml into a 25 $cm^2$ tissue culture flask, in the presence or the absence of 12459 (0.5 μM), cultured for 4 days, then trypsinized and counted. At each passage, $15 \times 10^3$ cells/ml were replated onto a new culture flask with fresh medium containing drug solution. Results were expressed as the cumulated population doubling (PD) as a function of the time of culture as previously described (17).

### Detection of SA β-galalactosidase activity

At 4 and 7 days after plating on 24-well microplate in the presence of 0.1 to 10 μM 12459, the endogenous senescence-associated β-galactosidase activity was assessed by a staining using X-Gal (5-bromo-4-chloro-3-indolyl-ß-D-galactopyranoside) as described previously (28).

β-galactosidase activity was also evaluated at day 20 for long-term culture with 0.5 μM 12459. The culture plates were placed on the stage of an inverted microscope (Nikon TE300) and observed at 20× magnification. Images were recorded as a 650 × 515 array with a CCD cooled camera (Coolsnap, Ropper Scientific).

### Western blot analysis

All experiments were performed with cells in a logarithmic phase by controlling the plating density. Cells were washed with ice-cold PBS and lysed in RIPA buffer (50 mM Tris–HCl (pH 7.4), 0.25% sodium desoxycholate, 150 mM NaCl, 1 mM EDTA, and 1 mM PMSF), including a protease inhibitor cocktail at 1 μg/ml (Mini complete protease, Roche Diagnostics). After 30 min on ice, lysates were cleared by centrifugation. Protein concentration was routinely measured with the Bio-Rad protein assay. Cell lysates containing equal amounts of total protein (25–40 μg) were resolved on a 12% or 10% SDS–PAGE, transferred to a PVDF membrane (Macherey-Nalgel) by electroblotting in 25 mM Tris (pH 8.3), and 192 mM glycine. Membranes were blocked for 3 h at room temperature in 10 mM Tris (pH 7.5) containing 0.15 M NaCl, 0.1% Tween-20 and 5% non-fat dry milk. Primary and secondary immunodetection, as well as washes, were performed in the same buffer using 5% dry milk. Western blot analysis was accomplished according to standard procedure using SuperSignal West Pico chemiluminescent substrate (Pierce). The following primary antibodies were used (1:1000 unless otherwise indicated): Monoclonal antibody to active Caspase 3 (Imgenex), Monoclonal anti-β-actin clone AC-15 (1:10 000) and anti-Bcl-2 clone 100 (Sigma), monoclonal anti-cleaved PARP asp 214 (Cell signalling) and anti-Bax (Santa Cruz).

### Mitochondrial membrane potential ($\Delta\psi_m$) and Reactive Oxygen Species (ROS) production

Fluorescence from JC1 monomers (green) and J-aggregates (red) was specific to the mitochondrial membrane potential ($\Delta\psi_m$) state (low and high, respectively). Therefore, the red/green fluorescence intensity ratio allowed the characterization of mitochondrial function. After washing twice, JC-1 emission was recorded by spectrofluorimetry to follow the quantitative evolution of ($\Delta\psi_m$) in treated cells compared with control cells. Cells were seeded into 25 $cm^2$ tissue culture flasks. After 24 h, cells were treated with appropriate concentrations of 12459 for different incubation times. The cells were washed and labeled with 3 μM JC1 in 5 ml final volume for 45 min. Cells were then trypsinized and resuspended in 2 ml RPMI without phenol red for spectrofluorimetric analysis using 488 nm as excitation wavelength. Relative membrane potential was expressed as: $(I_{590\ nm}/I_{530\ nm} + I_{590\ nm}) \times 100$. The protonophore carbonyl cyanide *m*-chlorophenylhydrazone (CCCP, Sigma) was used as positive control for potential disruption.

ROS production was determined using carboxy fluorescein-AM (CF). After cell treatment, 5 μM CF was added to 5 ml final volume for 30 min. Trypsinized cells were then analyzed by spectrofluorimetry using 488 nm for excitation and 515 nm for fluorescence emission measurement.

### Solution hybridization experiments

The non-denaturing hybridization assay to detect the 3′ telomere G-overhang was performed as described previously (27). A total of 2.5 μg aliquots of undigested genomic DNA was hybridized at overnight 50°C with 0.5 pmol of [γ−$^{32}$P]ATP-labeled (5′-CCCTAA-3′)$_4$ oligonucleotide (21C) in sodium hybridization buffer (10 mM Tris–HCl (pH 7.9), 50 mM NaCl, and 1 mM EDTA) in a volume of 20 μl. For competition with Pu22myc (5′-GAGGGTGGGGAGGGTGGGGAAG-3′) the reactions were performed in the presence of 10 μM Pu22myc. Reactions were stopped by the addition of 6 μl of loading buffer (20% glycerol, 1 mM EDTA, and 0.2% bromophenol blue). Hybridized samples were size-fractionated on 0.8% agarose gels in 1× TBE buffer containing ethidium bromide (EtBr). Gels were dried on Whatman filter paper. Ethidium fluorescence and radioactivity were scanned in a phosphorimager (Typhoon 9210, Amersham). The procedure

allows detection of the amount of single-strand overhang available for hybridization. Results were expressed as the relative hybridization signal normalized to the fluorescent signal of EtBr.

### Real-time PCR analysis

Total RNA was isolated from $1 \times 10^6$ cells using RNeasy Mini Kit (Quiagen).An aliquot of 1 μg RNA was reverse transcribed using a reverse transcription kit (Promega). Real-time PCR was performed with QuantiTect™ SYBR-Green PCR Kit (Quiagen) on the Lightcycler™ system (Roche diagnostics). The expression level of Bax and Bcl-2 were normalized by 18S ribosomal RNA level of the same sample. Reaction mixtures contained 10 μl of 2× Quantitect SYBR-Green PCR Master Mix, 2 μl of reverse-transcriptase-generated cDNA in a final volume of 20 μl containing primers (Proligo, Paris, France) at 125 nM. The primer sequences for *18S ribosomal RNA* gene were: 5′-CCCTCCAATGGATCCTCGTT-3′ for the forward primer, and 5′-AGTGACGAAAAATAACAATACAGGACTCT-3′ for the reverse primer. The primer sequences for Bax were: 5′-TTCCGAGTGGCAGCTGACAT-3′ for the forward primer, and 5′-TTCCAGATGGTGAGTGAGGC-3′ for the reverse primer. The primer sequences for Bcl-2 were: 5′-GGTGAACTGGGGGAGGATTGT-3′ for the forward primer, and 5′-CTTCAGAGACAGCCAGGAGAA-3′ for the reverse primer. After an initial incubation step at 95°C for 8 min, 25–30 PCR cycles were performed. The cycling conditions consisted of a denaturation at 95°C for 10 s, annealing either at 60°C for 5 s for 18S and Bax, or at 58°C for Bcl-2 and extended at 72°C for 7 s. To confirm amplification specificity, the PCR products were subjected to a melting curve analysis. Relative gene expression was expressed as a ratio of the expression level of the gene of interest to that of *18S ribosomal RNA*, with values in untreated A549 cells defined as 100%.

## RESULTS

### 12459 induces delayed apoptosis mediated by the mitochondrial pathway

We have previously shown that the triazine derivative 12459 (Figure 1a) has a dose-dependent dual antiproliferative effect on the A549 human tumor cell line (17). Apoptosis occurred after short-term treatments with concentrations >4 μM and a senescence-like delayed growth arrest was observed after long-term treatments with concentrations <1 μM (17,18). A characteristic feature of the short-term effect of 12459 on A549 cells is a delayed action, since both antiproliferative effects and final morphological changes associated with apoptosis were observed at 48 h. As shown in Figure 1b, a significant decrease in A549 cell proliferation was observed at 48 h but not at 24 h in the presence of 10 μM 12459. In agreement, nuclear morphological changes characterizing apoptosis were detected after 48 h and reached 20% of the total cells at day 4 (Figure 1c). Therefore, 12459-induced apoptosis presents a significant and characteristic delay, as compared with other well known antitumor agents, such as camptothecin.

In order to further characterize the apoptotic response triggered by 12459, we have also used A549 cells with an acquired resistance to 12459. The resistant clones JFD18 and JFD9 were obtained after an EMS mutagenesis and a soft agar cloning in the presence of 10 μM 12459 (25). In agreement with the delayed apoptotic response induced by 12459, differences in the cell viability characterizing the resistance of these clones were observed after a 48 h delay (Figure 1b).

JFD clones were also found to be resistant to 12459-induced apoptosis, as evaluated by Hoechst staining. Apoptotic nuclear bodies were observed in 5–8% of resistant JFD18 and JFD9 cells, as compared to 20% of sensitive A549 cells after 96 h of drug treatment with 10 μM 12459 (Figure 1c), thus indicating a steep decrease in the final steps of the apoptotic pathway.

The resistance to 12459 might represent upstream processes such as accessibility to the ligand, modifications of the intracellular targets, or direct relationship to the final apoptotic pathway itself. We have previously shown that the expression of the multidrug resistant factors (MDR1, MRP1, MRP2, MRP3 and BCRP) was not modified in these resistant clones [(25) and data not shown]. Telomerase, which is thought to be one of the intracellular targets of this G-quadruplex ligand, was found to be overexpressed in JFD18 cells but remained at a normal level in JFD9 cells (25,26), suggesting that additional mechanisms might be involved in 12459 resistance.

We have examined here some of the characteristics of the apoptotic pathway induced by 12459. The expression of anti- or pro-apoptotic proteins belonging to the Bcl-2 family is known to determine events associated with the mitochondrial onset of apoptosis. Western blot analysis indicated a significant increase of Bax after 24 h of 12459 treatment (Figure 2b); and under the same conditions, a decrease of Bcl-2 was observed after 48 h of drug treatment (Figure 2a and b). Similar results were found at the transcriptional level by using quantitative RT–PCR analysis (Figure 2c and d). An alteration in the Bcl-2/Bax balance at both protein and mRNA levels was provoked by 12459, as previously reported for DNA damaging agents (29).

Western blot analysis indicated that Bax protein levels were unchanged in untreated JFD18 and JFD9 clones, as compared with A549 cells (Figure 2b). In addition, 12459-induced overexpression of Bax was not modified in these clones after 24 and 48 h of drug treatment. In contrast, the Bcl-2 protein level was increased in untreated JFD9 and JFD18 clones (Figure 2b). Furthermore, JFD18 and JFD9 cells maintained a high level of Bcl-2 under 12459 treatment. Quantitative RT–PCR analysis of the transcripts of these genes confirmed these findings at the transcriptional level (result not shown) and suggested that activation of Bcl-2 activation, and not of Bax, is associated with the resistance phenotype.

We also studied the time course of caspase-3 activation. Western blot analysis revealed a delayed and time-dependent appearance of the active proteolytic fragment of caspase-3, which was detected after 36 h of treatment with 12459 (Figure 3b, see also Figure 4c). In agreement, caspase degradation of the native 116 kDa PARP yielding a 89 kDa proteolytic fragment was evident after 36 h of treatment with 12459 (Figure 3a, see also Figure 4b). In contrast, the activation of caspase-8, which is involved in the death receptor pathway of apoptosis, was very low and remained at background levels under 12459 treatment (result not shown). In addition, 12459-induced apoptosis was inhibited in the presence of the DEVD-FMK caspase-3 inhibitor but not with the IETD-FMK caspase-8 inhibitor (Figure 3c), suggests that 12459 triggers

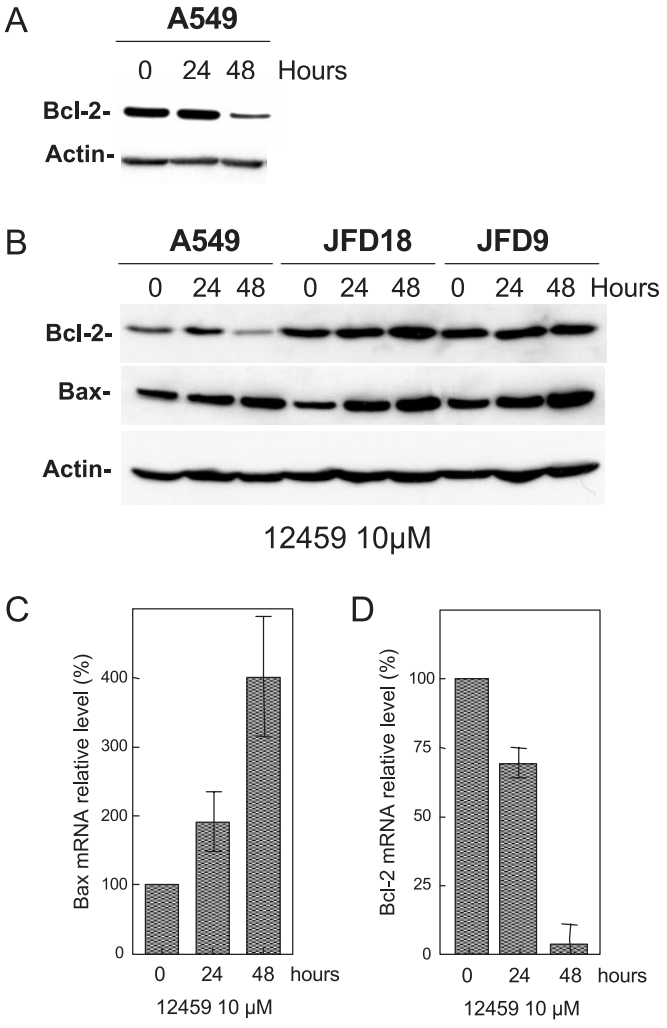


**Figure 2.** (**a** and **b**) Western blot analysis of Bcl-2 and Bax protein expression performed in A549, JFD18 or JFD9 control cells (0) or cells treated with 10 µM 12459 for 24 or 48 h, as indicated. β-actin was used as a control for protein loading. (**c** and **d**) Analysis of Bcl-2 and Bax mRNA expression by quantitative RT–PCR in untreated A549 cells (0) and in A549 cells treated with 10 µM 12459 for 24 or 48 h. Results (mean ± SD of triplicates) were normalized relative to 18S ribosomal RNA level, and expressed relative to untreated A549 cells, defined as 100%, as described in Materials and Methods.

the apoptotic cascade essentially through the mitochondrial pathway.

PARP cleavage was also found to be significantly reduced in JFD resistant clones, as compared to sensitive A549 cells (Figure 3a). Taken together, these results indicate that the resistant phenotype of these clones is associated with a reduction of apoptosis.

We also observed a time-dependent decrease of the mitochondrial membrane potential to 75% of control after 12 h of treatment and to 28% of control after 6 h of treatment with 1 and 10 µM 12459, respectively (Figure 3d). Interestingly and despite the delay of the final onset of the apoptotic cascade (>36 h), such an effect upon mitochondria reflects a rapid action of the compound that might be related to consequences of its action on cellular DNA. An increase in ROS was also induced by 12459 that was detectable after 4 h of treatment in A549 cells (Figure 3e). The maximal increase in ROS (100%) was observed after 8 h of treatment (Figure 3e).

Together, our results indicate that 12459 induces a delayed apoptosis (>36 h) mediated by caspase effectors after an early mitochondrial response and that the resistant phenotype of the JFD clones is associated with a reduction of apoptosis which involves an activation of Bcl-2.

### Bcl-2 overexpression induces apoptotic resistance to 12459

To determine whether the Bcl-2 overexpression is directly related to the resistance phenotype, we transfected A549 cells with an expression vector containing Bcl-2 cDNA under the cytomegalovirus (CMV) promoter (pCDNA3Bcl-2). After 3 weeks of selection, a stable A549::Bcl-2 transfected cell line was established that presented a 10-fold overexpression of the Bcl-2 protein, as determined by western blot analysis (Figure 4a).

Cell viability experiments indicated a marked and delayed resistance of the transfected cell line to the effect of 12459. A resistance was observed after a 48-h drug treatment for 10 and 20 µM 12459, and after 72 h for 5 µM (Figure 4d). In addition, PARP cleavage was found to be significantly reduced in A549::Bcl-2 cells treated with 10 µM 12459 since only a faint cleavage was detected after a 48-h treatment, as compared to A549 parental cells (Figure 4b). Similar results were found for caspase 3 cleavage (Figure 4c). These data indicate that the overexpression of Bcl-2 in A549 cells is sufficient to confer a resistance to the apoptotic effect of 12459. Therefore, overexpression of Bcl-2 in JFD clones is likely to represents a modification of the apoptotic pathway involved in the resistance to this ligand.

### Bcl-2 overexpression is not sufficient to confer resistance to senescence induced by long-term treatment with 12459

Previous studies have indicated that G-quadruplex ligands can induce a senescence-like phenotype, in which cells arrest their growth and display important morphological modifications, associated with the expression of SA β-galactosidase activity (17,22,30). Such phenotype has been previously characterized during long-term treatment with low concentrations of 12459 and was associated with telomere shortening (17). Whether higher concentrations of 12459 and shorter exposures could induce senescence, also representing an alternative to the apoptotic death of the cells, has not been evaluated. We have therefore studied the appearance of these senescent cells in both A549 and A549::Bcl-2 cell lines for 12459 concentrations ranging from 0.1 to 10 µM and up to 7 days of drug treatment. SA β-galactosidase positive cells were observed after a four day delay, with 12459 concentrations as low as 0.3 µM in both A549 and Bcl-2 transfected cells (Figure 5a). However, the amount of SA β-galactosidase positive cells remained unchanged for A549 and A549::Bcl-2 cell lines and corresponded to a small percentage of the treated-cell population (in the range of only 3–5%). After 7 days of treatment up to 10 µM, some SA β-galactosidase positive cells were still observed but represented a small proportion of the remaining cells, as compared to those undergoing apoptosis (Figure 5b). These results suggested that senescence induction is a minor

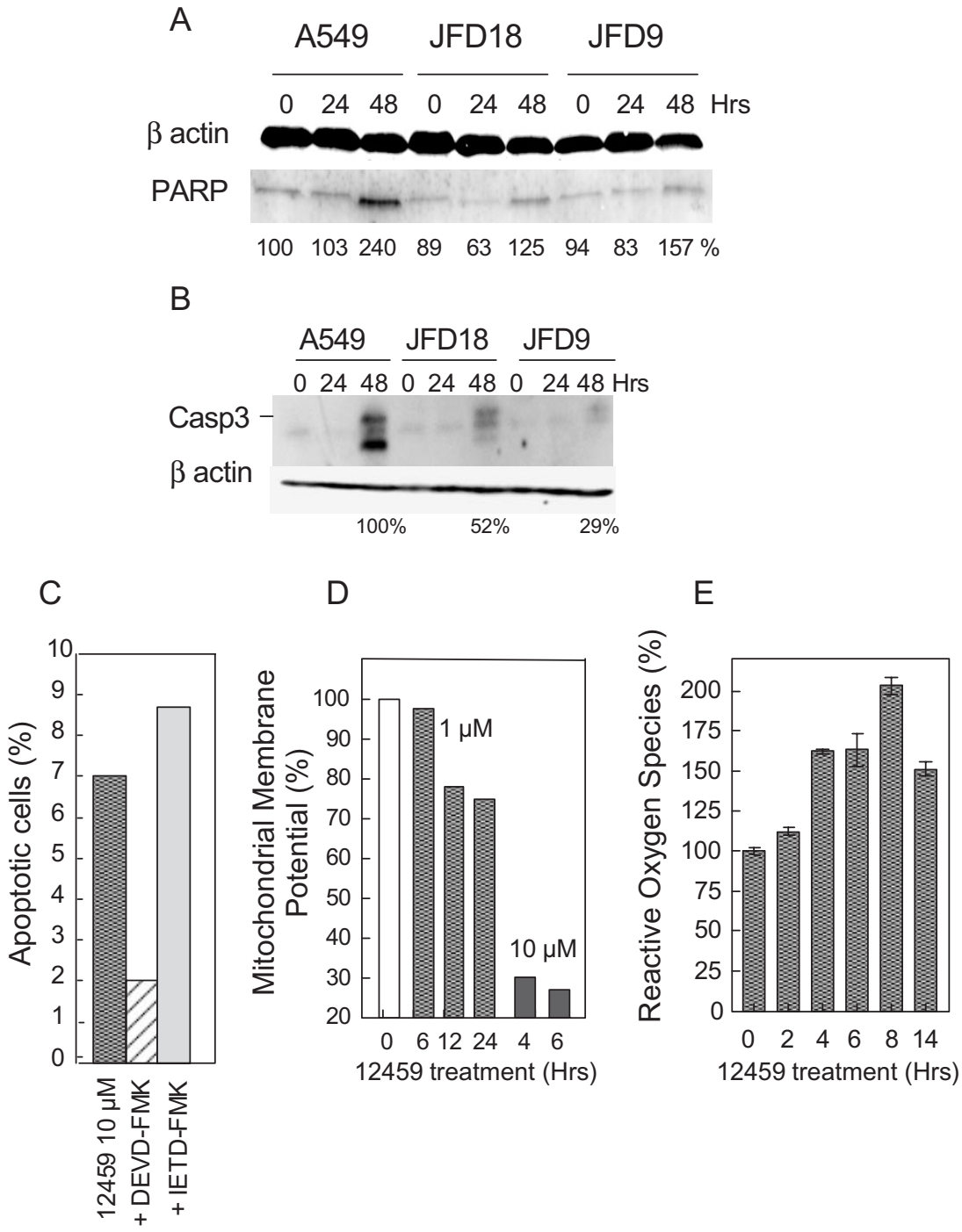


**Figure 3.** (**a** and **b**) Western blot analysis of PARP cleaved form (89 kDa) protein expression (a) or Caspase 3 cleaved form (17 kDa) protein expression (b) performed in untreated A549, JFD18 or JFD9 cells (0) and in cells treated with 10 μM 12459 for 24 or 48 h. β-actin was used as a control for protein loading. Relative PARP cleavage (a) or Caspase 3 cleavage (b) was measured by densitometry scanning of the films, normalized relative to β-actin protein expression and results were expressed relative to untreated A549 cells defined as 100% for PARP or relative to A549 cells treated for 48 h with 12459 for caspase 3 (see bottom of each panel). (**c**) Effect of caspase inhibitors on apoptosis induced by 12459 (10 μM, 48 h) on A549 cells. DEVD-FMK and IETD-FMK at 2 μM were added to 12459 and apoptosis was revealed by Hoechst 33342 staining. (**d**) Mitochondrial membrane potential was measured by spectrofluorimetry of the JC1 dye in A549 control cells (0) or in cells treated with 1 μM 12459 for 0, 6, 12 or 24 h or with 10 μM 12459 for 4 or 6 h, as described in Materials and Methods. (**e**) ROS were measured by spectrofluorimetry using carboxy fluorescein-AM in A549 control cells (0) or in cells treated with 10 μM 12459 for 2, 4, 6, 8 and 14 h. Results represent the mean ± SM of duplicate determinations.

event, as compared to the apoptosis induced by 12459 treatment at this concentration (10 μM).

Despite the small amount of cells in which senescence was induced, a long-term administration of 12459 at a sub-apoptotic concentration is able to induce cumulative events able to impair cell growth. To determine whether Bcl-2 overexpression is able to protect from the long-term effect of 12459, we have used 0.5 μM of the ligand,

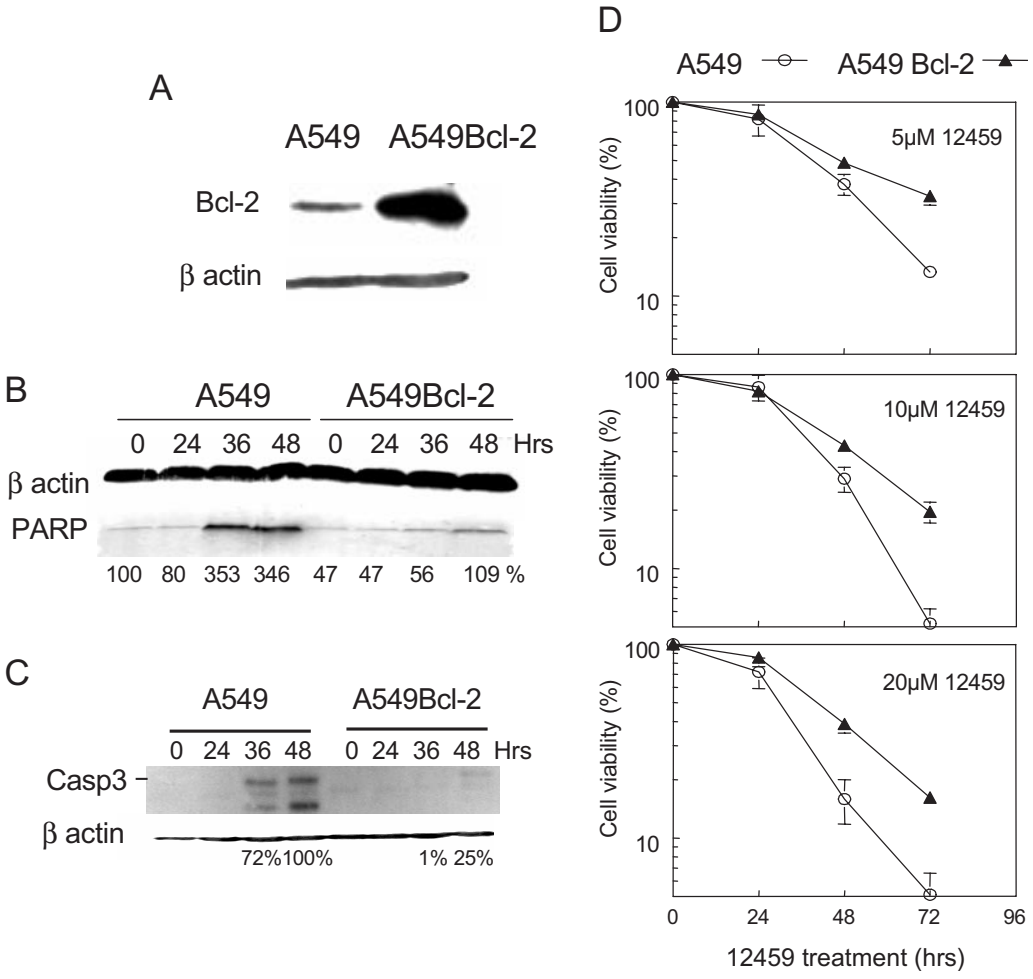


**Figure 4.** (**a**) Western blot analysis of Bcl-2 protein expression performed in A549 parental cells and A549 cells transfected by Bcl-2 (A549::Bcl-2). β-Actin was used as a control for protein loading. (**b** and **c**) Western blot analysis of PARP cleaved form (89 kDa) protein expression (b) or Caspase 3 cleaved form (17 kDa) protein expression (c) performed in untreated A549 and A549::Bcl-2 cells (0) and in cells treated with 10 μM 12459 for 24, 36 or 48 h. β-Actin was used as a control for protein loading. Relative PARP cleavage (b) or Caspase 3 cleavage (c) was measured by densitometry scanning of the films, normalized relative to β-actin protein expression. Results were expressed relative to untreated A549 cells defined as 100% for PARP, or relative to A549 cells treated for 48 h with 12459 for caspase 3 (see bottom of each panel). (**d**) Effect of 12459 (5, 10 and 20 μM) on the growth of human A549 lung carcinoma parental cells (open circle), and transfected A549::Bcl-2 cells (closed triangle) for the indicated times. Mean ± SD of three independent experiments.

a concentration able to induce senescence but unable to trigger apoptosis during short-term treatment of A549 and Bcl-2 transfected cells. In these conditions, A549 cells reached a growth plateau after 12 days and a complete growth arrest was observed after 20 days of treatment (Figure 6a). For A549::Bcl-2 cells, although a significant resistance was observed after 4 days, the complete growth arrest of the culture was also observed after 20 days of treatment. At this time, the proportion of SA β-galactosidase cells was also found to be identical in A549- and A549::Bcl-2-treated cells (Figure 6b).

These experiments indicate that Bcl-2 overexpression is not sufficient to confer resistance to long-term treatment with 12459.

### 12459 induces an alteration of the telomeric G-overhang

Recent studies with telomestatin indicated that the telomeric G-overhang represents one of the direct targets of this ligand. We have determined here the effect of 12459 on the telomeric G-overhang from A549 and A549::Bcl-2 cell lines. Hybridization of a telomeric C-rich probe (21C) under non-denaturing conditions allowed the measurement of the single-stranded G-overhang signal in undigested genomic DNA samples (27). A quantification relative to the EtBr staining of total genomic DNA indicated that the G-overhang hybridization signal was similar in A549 and Bcl-2 transfected cells (Figure 7a and b). Treatment of A549 cells with 10 μM 12459 induced a decrease of the overhang signal to 50–55% of the control after 72 h (Figure 7a and b). An identical result was found in A549::Bcl-2 cells (Figure 7a and b), suggesting that the Bcl-2 overexpression has no influence on the action of 12459 at the telomeric ends. Interestingly, we noticed that 12459 had a very rapid effect on the telomeric overhangs of A549 cells since the decrease was detectable within 24 h of drug treatment.

Previous studies with telomestatin have shown that such a rapid decrease was on account of a tight binding of the

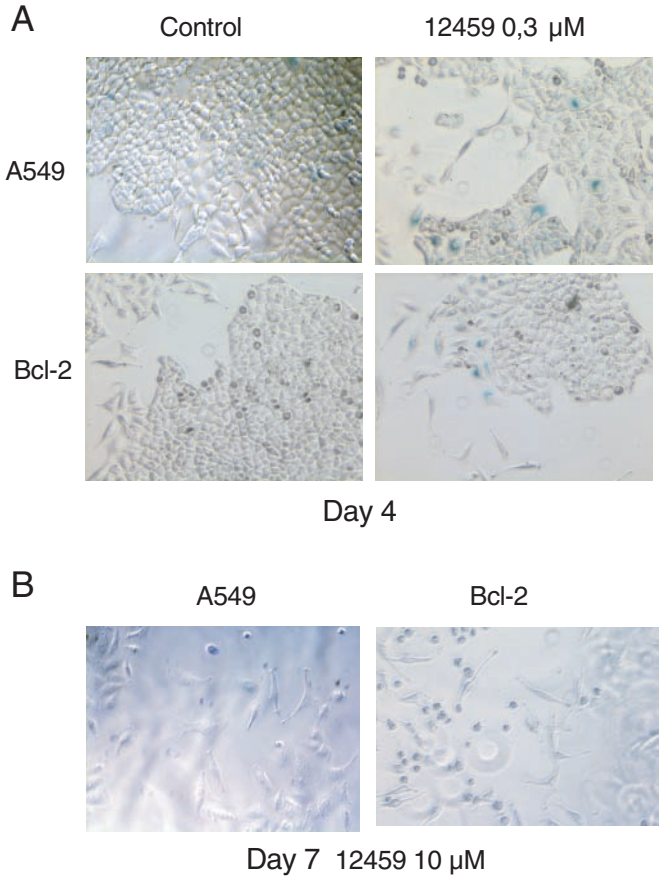


**Figure 5.** SA β-galactosidase activity in untreated A549 or A549::Bcl-2 cells (control) or in cells treated with 12459 for 4 days (0.3 µM, panel **a**) or for 7 days (10 µM, panel **b**). Observed by phase contrast microscopy, the cells with 4 days' treatment show the appearance of senescent β-galactosidase positive cells, while 7 days' treatment induces the appearance of round apoptotic cells.

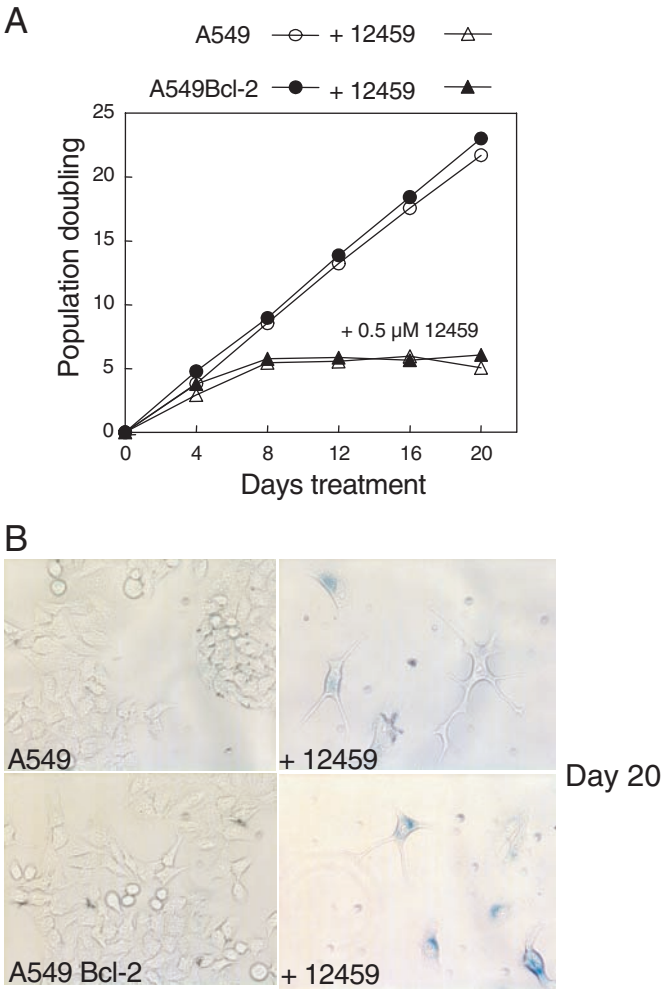


**Figure 6.** (**a**) Long-term proliferation curve of A549 or A549::Bcl-2 cells in the absence (open and closed circles, respectively) or presence of 12459 (0.5 µM) (open and closed triangles, respectively). A cell growth plateau appears at day 8 and cells enter senescence at day 20 for both 12459-treated cell lines at a population doubling equal to 5. (**b**) Expression of SA β-galactosidase activity in untreated A549 or A549::Bcl-2 cells (A549, A549Bcl-2) or in cells treated with 0.5 µM 12459 (+ 12459) for 20 days.

ligand to the telomeric overhangs, which is mediated by a G-quadruplex stabilization that further impairs the hybridization reaction (27). In order to distinguish between a degradation and a binding of 12459 to the telomeric overhangs, we have examined the *in vitro* effect of 12459 on the hybridization of the 21C probe to the telomeric overhangs from purified genomic DNA. Adding to the hybridization reaction an overnight incubation of up to 10 µM 12459 did not significantly inhibit the G-overhang signal (Figure 7d). A further increase of the 12459 concentration to 100 µM resulted in a complete inhibition of the probe hybridization to the telomeric overhangs (Figure 7d and e). Competition experiments with a *c-myc* promoter quadruplex (Pu22myc) that is efficiently stabilized by 12459 were used to investigate the mechanism of such hybridization inhibition (31). The addition of Pu22myc oligonucleotide to the reaction reversed most of the 12459-induced inhibition (Figure 7d and e). This suggested that 12459 is able to inhibit the hybridization reaction through the formation of G-quadruplexes at telomeric overhangs—as previously reported for telomestatin (27)—but at a higher concentration. Such differences between these two ligands could be explained, in part, by their potency to stabilize telomeric quadruplexes. FRET experiments showed that ΔTm is only 8°C for 12459 and >20°C for telomestatin (17,27).

The hybridization reaction of 21C to the telomeric overhang, in the presence of ligands, corresponded to a competition between 21C and ligands for the telomeric overhang. The resultant products of the reaction reflected the ability of 21C to destabilize telomeric G-quadruplexes as well as to form a duplex. In the absence of ligands, such equilibrium was in favour of the duplex formation as previously reported for oligonucleotides (32). Our result suggests that 12459 induces much less stable G-quadruplexes than telomestatin at telomeres.

In the presence of 10 µM Pu22myc competitor, the hybridization reaction on DNA samples from 12459-treated A549 cells did not display a reversion of the G-overhang signal decrease (Figure 7c). Therefore, we conclude that the G-overhang signal loss in 12459-treated A549 cells corresponds to an effective degradation of the telomeric G-overhang.

Interestingly, the G-overhang degradation seems to correlate with the appearance of the apoptosis in A549 and is also observed in Bcl-2 transfected cells. This would suggest that

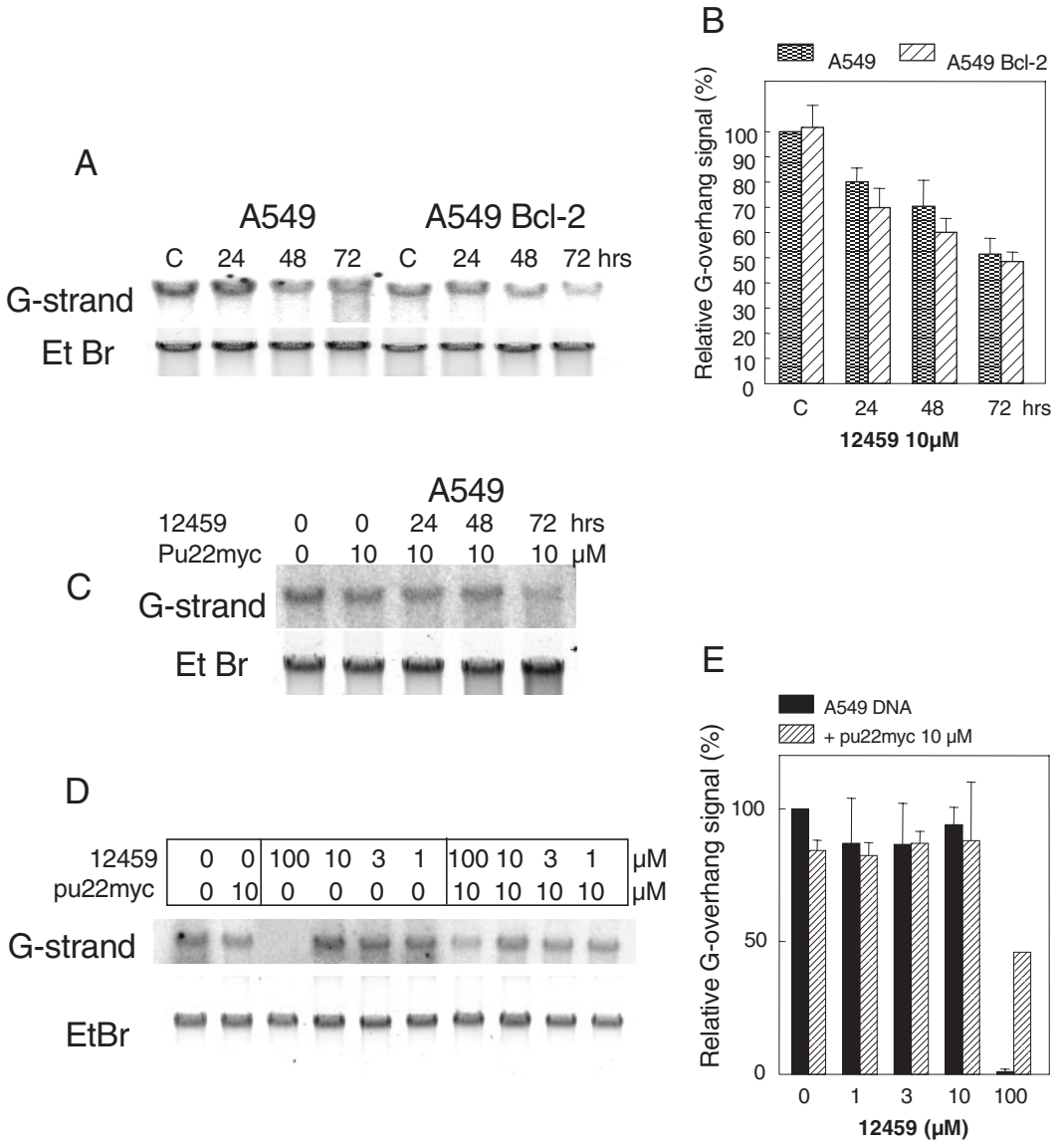


**Figure 7.** (**a**) Non-denaturing solution hybridization analysis of the 3′ telomeric overhang in A549 or A549::Bcl-2 control cells (C) or in cells treated with 10 μM 12459 for 24, 48 or 72 h, as indicated. G-strand hybridization signal of the gel with 21C telomeric probe and EtBr staining of the gel. (**b**) Quantification of the 12459 effect. G-overhang hybridization signal is normalized relative to the EtBr signal. The results are expressed relative to untreated A549 DNA (defined as 100%) and corresponded to mean ± SD of triplicate independent experiments including data presented in panel a (**c**) Non-denaturing solution hybridization analysis of the 3′ telomeric overhang in A549 control cells (0) or cells treated with 10 μM 12459 for the indicated time, in the absence (0) or in the presence of 10 μM Pu22myc quadruplex competitor (10). The addition of Pu22myc does not inhibit the 12459-induced decrease of the G-strand signal at 72 h (compare with panel a). (**d**) Non-denaturing solution hybridization analysis of the telomeric G-overhang from purified A549 DNA treated with different concentrations of 12459 (100, 10, 3, 1 μM) in the presence or the absence of 10 μM Pu22myc quadruplex competitor, as indicated at the top of the panel. (**e**) Quantification of the effect of 12459 *in vitro*. G-overhang hybridization signal is normalized relative to the EtBr signal. The results are expressed relative to untreated A549 DNA (defined as 100%) and corresponded to mean ± SD of three independent experiments, including data presented in panel d.

the G-overhang degradation is an early event uncoupled from the apoptotic processes. However, that apoptosis could trigger the degradation of the telomeric ends through the liberation of nucleases during the final stages of nuclear fragmentation cannot be excluded. We, therefore, used camptothecin to induce apoptosis in A549 cells in order to examine the status of the telomeric G-overhang. Treatment of A549 cells for 24 h with up to 5 μM camptothecin induced a significant apoptotic process with caspase activation, chromatin condensation and formation of nuclear bodies (Figure 8c) but did not generate any significant decrease of the telomeric G-overhang signal (Figure 8a and b). This result suggests that the G-overhang degradation is a process selectively induced by 12459 at telomeric ends that is not observed during the apoptotic response to camptothecin.

## DISCUSSION

The induction of replicative senescence has been described as one of the characteristics of G-quadruplex ligands. It is now well established that different series of G-quadruplex ligands, including 12459, telomestatin, BRACO-19 and RHSP4 induce

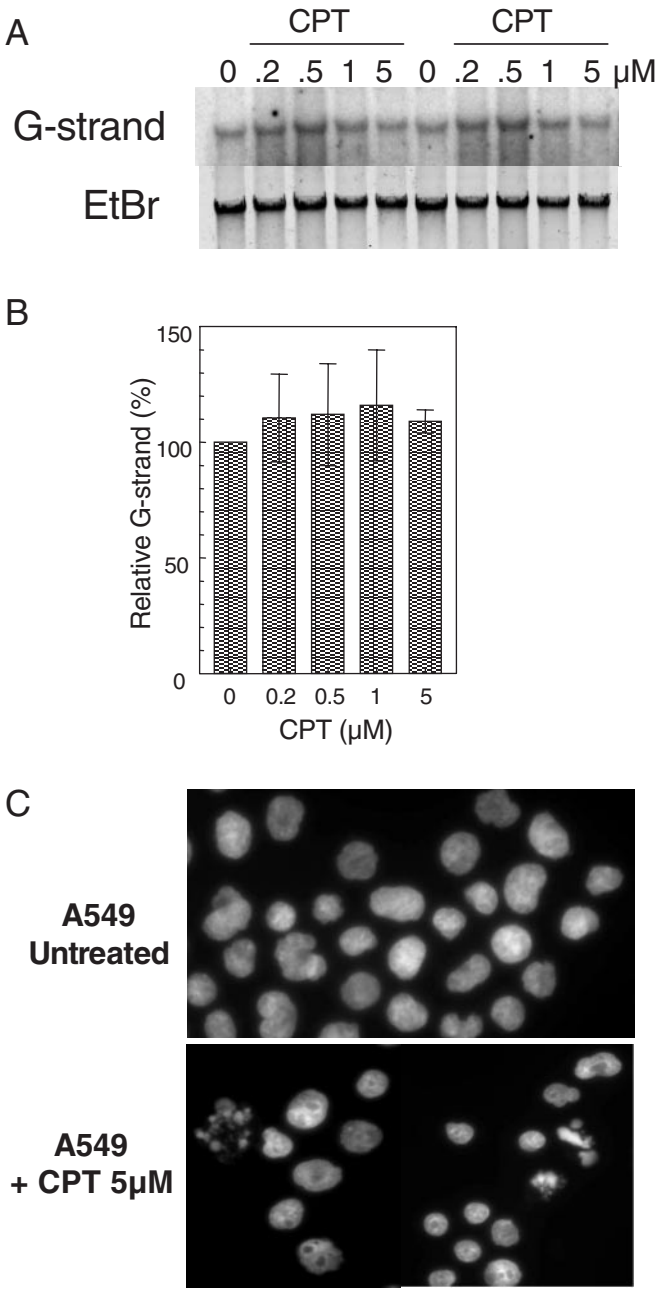


**Figure 8.** (**a**) Non-denaturing solution hybridization analysis of the 3′ telomeric overhang in untreated A549 cells untreated (0) or in cells treated with 0.2, 0.5, 1 or 5 μM camptothecin (CPT) for 48 h (duplicate loading of a representative experiment). G-strand, hybridization signal of the gel with 21C telomeric probe and EtBr staining of the gel. (**b**) Quantification of the CPT effect. G-overhang hybridization signal is normalized relative to the EtBr signal. The results are expressed relative to untreated A549 DNA (defined as 100%) and corresponded to the mean ± SD of two independent experiments in duplicate. (**c**) Apoptosis induction by CPT (5 μM) in A549 cells after 48 h of treatment (A459 + CPT 5 μM). Cells were fixed and stained with DAPI and examined for nuclei morphology under fluorescence microscopy using an Axiovert 200M inverted microscope (Zeiss) equipped with a 40× objective.

the appearance of positive β-galactosidase cells and telomere shortening after a long-term treatment of a range of tumor cell lines (19,21–24,30,33,34). We also show here that 12459 induces the appearance of senescent cells after short-term treatment, in agreement with previous findings with RHSP4 and BRACO-19 (22,30). However, these senescent cells represent only a small percentage of the cell population. This suggests that senescence induction is not the major mechanism responsible for the short-term biological effect of these ligands.

Besides senescence, apoptosis was also observed after treatment with these G-quadruplex ligands. A characteristic feature of this apoptosis is its delayed appearance varying as a function of the ligand and the cell line used. Recent studies with RHSP4, telomestatin and 307A showed that apoptosis occurred after a 5–12 day delay (22,33–35). Although not formally shown, the *in vivo* antitumor effect of BRACO-19 against UXF1138L xenograft is compatible with a rapid apoptotic tumor kill response (36). We demonstrate here that 12459 induces apoptosis after a 48-h delay for high drug concentrations (>5 μM). The apoptotic pathway generated by 12459 is characterized by a dysfunction of the Bcl-2/Bax balance, caspase 3 and PARP cleavage, suggesting that this ligand triggers the mitochondrial apoptotic pathway. We also show here that for short-term treatment, apoptosis predominates over the appearance of senescent cells, this result represents the most striking difference from other G-quadruplex ligands described, which needed a longer delay to achieve massive apoptosis(22,33–35).

Previous findings indicated that JFD clones resistant to the apoptotic effect of 12459 displayed telomere capping alterations (25). We show here that these clones present an overexpression of the anti-apoptotic protein Bcl-2. In addition, A549 cells transfected with Bcl-2 show a resistance to the apoptotic action of 12459. This correlates with a delayed activation of the mitochondrial apoptotic cascade (PARP and Caspase 3 cleavage), indicating that Bcl-2 is one of the determinants of the apoptotic resistance to this ligand.

Interestingly, we demonstrate that Bcl-2 overexpression is not sufficient to confer resistance to the long-term effect of 12459. The Bcl-2-transfected A549 cell line entered into a senescent growth arrest in a similar manner to parental A549 cells. These data suggest that senescence, which is not predominant for 12459 short-term treatment, becomes a critical determinant for responses to a prolonged treatment with this ligand, as previously reported, under treatment with other anticancer therapies (37). Thus, we also conclude that G-quadruplex ligand-directed senescence is uncoupled from apoptosis.

However, since Bcl-2 is a downstream mitochondrial effector, and because of the rapid onset of apoptosis by this 12459, the relationship between the short-term effect of this ligand and its molecular action against telomeres becomes questionable.

It has been hypothesized that the induction of a quadruplex structure at the end of the telomeric G-overhang results in telomere uncapping (6). End-to-end chromosomal fusions or anaphases bridges, consistent with this hypothesis, have been reported for G-quadruplex ligands (22,30,35). A recent report from our group also indicated that telomestatin directly interacts with the telomeric G-overhang from A549 cells and induced its degradation concomitantly with the delayed loss of cell viability (27). We have shown here that 12459 presents a major difference with telomestatin as it induced a rapid degradation of the telomeric G-overhang that paralleled the induction of apoptosis in A549 cells.

Since the telomeric G-overhang degradation paralleled the apoptotic response of A549 cells to 12459, such a degradation might reflect a telomeric damage response to 12459 associated with the final growth arrest of the cells. On the other hand, the G-overhang degradation could be a consequence of the nuclease release from apoptotic cells. Our results present two pieces of evidence that the G-overhang degradation rather reflects a specific telomeric response to 12459. First, the over-expression of Bcl-2 that counteracts the apoptosis induced by 12459 is not able to modify the G-overhang degradation mediated by 12459. Second, the antitumor agent camptothecin is not able to trigger the G-overhang degradation in conditions that induce a massive apoptosis.

Interestingly, the G-overhang degradation was detected within 24 h of treatment, suggesting that this response to the ligand precedes the onset of the final apoptotic cascade. However, 12459 is able to trigger other rapid cellular events, such as a decrease of the mitochondrial membrane potential and an increase of ROS within few hours. Preliminary studies also indicate that 12459 treatment triggers a p53 response detectable in <6 h (C. Douarre, unpublished results). Whether these events are associated with the loss of the telomeric overhang remains to be determined. Although the combined effect of ROS and 12459 involved in the G-overhang loss could not be excluded, the effects of ROS alone are unlikely to explain it since campthothecin, a known activator of ROS (38), does not alter the G-overhang. Future work will aim at determining the importance of this early cellular response in triggering events involved in the G-overhang degradation.

Finally, G-overhang degradation under the 12459 treatment would reflect the uncapping of the telomeric ends and represent the alteration of the binding of specific telomeric factors or effectors of the G-overhang during the replication. It is noteworthy that dominant negative TRF2 mimics the effect of a G-quadruplex ligand; and since TRF2 is involved in the formation of the T-loop, it is possible that 12459 alters such a telomeric structure or impairs the transitions between linear and T-loop states mediated by telomeric proteins (9).

In conclusion, our results demonstrate that the G-quadruplex ligand 12459 induces a delayed apoptosis involving the mitochondrial pathway and that this ligand is effective in the long-term independent of the Bcl-2 status of the cells. Its biological effect is associated with a specific degradation of the telomeric overhang. This finding supports the notion that alteration of telomeric ends is one of the main consequences of the intracellular action of G-quadruplex ligands.

## ACKNOWLEDGEMENTS

The authors wish to thank J.L. Mergny and E. Segal for helpful discussion, T. Wenner and C. Morrison for critical reading of the manuscript. The pcDNA3Bcl-2 vector is a kind gift from L. Debussche and M.N. Mary (Sanofi-Aventis, Vitry-sur-Seine, France). This work was supported by the 'Ligue Nationale contre le Cancer, Comités de la Marne et de la Haute Marne' and by the 'Association pour la Recherche contre le Cancer', grant no. 3644. C.D. is supported by a student fellowship from 'l'Association Régionale pour l'Enseignement et la Recherche Scientifique et technologique ARERS and by the 'Ligue contre le Cancer, Comité de l'Aisne'. Funding to pay the Open Access publication charges for this article was provided by the University of Reims.

*Conflict of interest statement*. None declared.

## REFERENCES

1. Blackburn,E.H. (2001) Switching and signaling at the telomere. *Cell*, **106**, 661–673.
2. McEachern,M.J., Krauskopf,A. and Blackburn,E.H. (2000) Telomeres and their control. *Annu. Rev. Genet.*, **34**, 331–358.
3. Shay,J.W. and Wright,W.E. (2002) Telomerase: a target for cancer therapeutics. *Cancer Cell*, **2**, 257–265.
4. Hahn,W.C., Counter,C.M., Lundberg,A.S., Beijersbergen,R.L., Brooks,M.W. and Weinberg,R.A. (1999) Creation of human tumour cells with defined genetic elements. *Nature*, **400**, 464–468.
5. Lavelle,F., Riou,J.F., Laoui,A. and Mailliet,P. (2000) Telomerase: a therapeutic target for the third millennium? *Crit. Rev. Oncol. Hematol.*, **34**, 111–126.
6. Neidle,S. and Parkinson,G. (2002) Telomere maintenance as a target for anticancer drug discovery. *Nature Rev. Drug Discov.*, **1**, 383–393.
7. Makarov,V.L., Hirose,Y. and Langmore,J.P. (1997) Long G tails at both ends of human chromosomes suggest a C strand degradation mechanism for telomere shortening. *Cell*, **88**, 657–666.
8. Wright,W.E., Tesmer,V.M., Huffman,K.E., Levene,S.D. and Shay,J.W. (1997) Normal human chromosomes have long G-rich telomeric overhangs at one end. *Genes Dev.*, **11**, 2801–2809.
9. Smogorzewska,A. and de Lange,T. (2004) Regulation of telomerase by telomeric proteins. *Annu. Rev. Biochem.*, **73**, 177–208.
10. Griffith,J.D., Comeau,L., Rosenfield,S., Stansel,R.M., Bianchi,A., Moss,H. and de Lange,T. (1999) Mammalian telomeres end in a large duplex loop. *Cell*, **97**, 503–514.
11. Blackburn,E.H., Chan,S., Chang,J., Fulton,T.B., Krauskopf,A., McEachern,M., Prescott,J., Roy,J., Smith,C. and Wang,H. (2000) Molecular manifestations and molecular determinants of telomere capping. *Cold Spring Harb. Symp. Quant Biol.*, **65**, 253–263.
12. Li,G.Z., Eller,M.S., Firoozabadi,R. and Gilchrest,B.A. (2003) Evidence that exposure of the telomere 3′ overhang sequence induces senescence. *Proc. Natl Acad. Sci. USA*, **100**, 527–531.
13. Duan,W., Rangan,A., Vankayalapati,H., Kim,M.Y., Zeng,Q., Sun,D., Han,H., Fedoroff,O.Y., Nishioka,D., Rha,S.Y. *et al.* (2001) Design and synthesis of fluoroquinophenoxazines that interact with human telomeric G-quadruplexes and their biological effects. *Mol. Cancer Ther.*, **1**, 103–120.
14. Karlseder,J., Smogorzewska,A. and de Lange,T. (2002) Senescence induced by altered telomere state, not telomere loss. *Science*, **295**, 2446–2449.
15. Davies,J.T. (2004) G-quartet 40 years later: from 5′-GMP to molecular biology and supramolecular chemistry. *Angew. Chem. Int. Edit.*, **43**, 668–698.
16. Mergny,J.L., Riou,J.F., Mailliet,P., Teulade-Fichou,M.P. and Gilson,E. (2002) Natural and pharmacological regulation of telomerase. *Nucleic Acids Res.*, **30**, 839–865.
17. Riou,J.F., Guittat,L., Mailliet,P., Laoui,A., Renou,E., Petitgenet,O., Megnin-Chanet,F., Hélène,C. and Mergny,J.L. (2002) Cell senescence and telomere shortening induced by a new series of specific G-quadruplex DNA ligands. *Proc. Natl Acad. Sci. USA*, **99**, 2672–2677.
18. Gomez,D., Aouali,N., Renaud,A., Douarre,C., Shin-Ya,K., Tazi,J., Martinez,S., Trentesaux,C., Morjani,H. and Riou,J.F. (2003) Resistance to senescence induction and telomere shortening by a G-quadruplex ligand inhibitor of telomerase. *Cancer Res.*, **63**, 6149–6153.
19. Kim,M.Y., Gleason-Guzman,M., Izbicka,E., Nishioka,D. and Hurley,L.H. (2003) The different biological effects of telomestatin and TMPyP4 can be attributed to their selectivity for interaction with intramolecular or intermolecular G-quadruplex structures. *Cancer Res.*, **63**, 3247–3256.
20. Nakajima,A., Tauchi,T., Sashida,G., Sumi,M., Abe,K., Yamamoto,K., Ohyashiki,J.H. and Ohyashiki,K. (2003) Telomerase inhibition enhances apoptosis in human acute leukemia cells: possibility of antitelomerase therapy. *Leukemia*, **17**, 560–567.
21. Gowan,S.M., Heald,R., Stevens,M.F. and Kelland,L.R. (2001) Potent inhibition of telomerase by small-molecule pentacyclic acridines capable of interacting with G-quadruplexes. *Mol. Pharmacol.*, **60**, 981–988.

22. Leonetti,C., Amodei,S., D'Angelo,C., Rizzo,A., Benassi,B., Antonelli,A., Elli,R., Stevens,M., D'Incalci,M., Zupi,G. *et al.* (2004) Biological activity of the G-quadruplex ligand RHPS4 is associated with telomere capping alteration. *Mol. Pharmacol.* **8**, 1063–1074.
23. Incles,C.M., Schultes,C.M., Kelland,L.R. and Neidle,S. (2003) Acquired cellular resistance to flavopiridol in a human colon carcinoma cell line involves up-regulation of the telomerase catalytic subunit and telomere elongation. Sensitivity of resistant cells to combination treatment with a telomerase inhibitor. *Mol. Pharmacol.*, **64**, 1101–1108.
24. Gowan,S.M., Harrison,J.R., Patterson,L., Valenti,M., Read,M.A., Neidle,S. and Kelland,L.R. (2002) A G-quadruplex-interactive potent small-molecule inhibitor of telomerase exhibiting *in vitro* and *in vivo* antitumor activity. *Mol. Pharmacol.*, **61**, 1154–1162.
25. Gomez,D., Aouali,N., Londono-Vallejo,A., Lacroix,L., Megnin-Chanet,F., Lemarteleur,T., Douarre,C., Shin-ya,K., Mailliet,P., Trentesaux,C. *et al.* (2003) Resistance to the short term antiproliferative activity of the G-quadruplex ligand 12459 is associated with telomerase overexpression and telomere capping alteration. *J. Biol. Chem.*, **278**, 50554–50562.
26. Gomez,D., Lemarteleur,T., Lacroix,L., Mailliet,P., Mergny,J.L. and Riou,J.F. (2004) Telomerase downregulation induced by the G-quadruplex ligand 12459 in A549 cells is mediated by hTERT RNA alternative splicing. *Nucleic Acids Res.*, **32**, 371–379.
27. Gomez,D., Paterski,R., Lemarteleur,T., Shin-Ya,K., Mergny,J.L. and Riou,J.F. (2004) Interaction of telomestatin with the telomeric single-strand overhang. *J. Biol. Chem.*, **279**, 41487–41494.
28. Dimri,G.P., Lee,X., Basile,G., Acosta,M., Scott,G., Roskelley,C., Medrano,E.E., Linskens,M., Rubelj,I., Pereira-Smith,O. *et al.* (1995) A biomarker that identifies senescent human cells in culture and in aging skin *in vivo*. *Proc. Natl Acad. Sci. USA*, **92**, 9363–9367.
29. Leung,L.K. and Wang,T.T. (1999) Differential effects of chemotherapeutic agents on the Bcl-2/Bax apoptosis pathway in human breast cancer cell line MCF-7. *Breast Cancer Res. Treat.*, **55**, 73–83.
30. Incles,C.M., Schultes,C.M., Kempski,H., Koehler,H., Kelland,L.R. and Neidle,S. (2004) A G-quadruplex telomere targeting agent produces p16-associated senescence and chromosomal fusions in human prostate cancer cells. *Mol. Cancer Ther.*, **3**, 1201–1206.
31. Lemarteleur,T., Gomez,D., Paterski,R., Mandine,E., Mailliet,P. and Riou,J.F. (2004) Stabilization of the c-myc gene promoter quadruplex by specific ligands inhibitors of telomerase. *Biochem. Biophys. Res. Commun.*, **323**, 802–808.
32. Phan,A.T. and Mergny,J.L. (2002) Human telomeric DNA: G-quadruplex, i-motif and Watson–Crick double helix. *Nucleic Acids Res.*, **30**, 4618–4625.
33. Shammas,M.A., Reis,R.J., Li,C., Koley,H., Hurley,L.H., Anderson,K.C. and Munshi,N.C. (2004) Telomerase inhibition and cell growth arrest after telomestatin treatment in multiple myeloma. *Clin. Cancer Res.*, **10**, 770–776.
34. Tauchi,T., Shin-Ya,K., Sashida,G., Sumi,M., Nakajima,A., Shimamoto,T., Ohyashiki,J.H. and Ohyashiki,K. (2003) Activity of a novel G-quadruplex-interactive telomerase inhibitor, telomestatin (SOT-095), against human leukemia cells: involvement of ATM-dependent DNA damage response pathways. *Oncogene*, **22**, 5338–5347.
35. Pennarun,G., Granotier,C., Gauthier,L.R., Gomez,D., Hoffschir,F., Mandine,E., Riou,J.F., Mergny,J.L., Mailliet,P. and Boussin,F.D. (2005) Apoptosis related to telomere instability and cell cycle alterations in human glioma cells treated by new highly selective G-quadruplex ligands. *Oncogene*, doi:10.1038/sj.onc.1208468.
36. Burger,A.M., Dai,F., Schultes,C.M., Reszka,A.P., Moore,M.J., Double,J.A. and Neidle,S. (2005) The G-quadruplex-interactive molecule BRACO-19 inhibits tumor growth, consistent with telomere targeting and interference with telomerase function. *Cancer Res.*, **65**, 1489–1496.
37. Roninson,I.B. (2003) Tumor cell senescence in cancer treatment. *Cancer Res.*, **63**, 2705–2715.
38. Palissot,V., Morjani,H., Belloc,F., Cotteret,S., Dufer,J. and Berchem,G. (2005) From molecular characteristics to cellular events in apoptosis-resistant HL-60 cells. *Int. J. Oncol.*, **26**, 825–834.